

Predicting the fatigue life of asphalt concrete using neural networks

J. Houlík^a, J. Valentin^a, V. Nežerka^{a,*}

^a*Faculty of Civil Engineering, Czech Technical University in Prague, Thákurova 7, 166 29 Praha 6, Czech Republic*

Abstract

Asphalt concrete's (AC) durability and maintenance demands are strongly influenced by its fatigue life. Traditional methods for determining this characteristic are both resource-intensive and time-consuming. This study employs artificial neural networks (ANNs) to predict AC fatigue life, focusing on the impact of strain level, binder content, and air-void content. Leveraging a substantial dataset, we tailored our models to effectively handle the wide range of fatigue life data, typically represented on a logarithmic scale. The mean square logarithmic error was utilized as the loss function to enhance prediction accuracy across all levels of fatigue life. Through comparative analysis of various hyperparameters, we developed a machine-learning model that captures the complex relationships within the data. Our findings demonstrate that higher binder content significantly enhances fatigue life, while the influence of air-void content is more variable, depending on binder levels. Most importantly, this study provides insights into the intricacies of using ANNs for modeling, showcasing their potential utility with larger datasets. The codes developed and the data used in this study are provided as open source on a GitHub repository, with a link included in the paper for full access.

Keywords: Asphalt concrete, Fatigue life, Binder content, Air voids, Machine learning

1. Introduction

Asphalt concrete (AC) is a composite material widely used in road construction. It consists of aggregates (crushed stone, gravel, or sand) and a bituminous binder, which is either used as paving-

*Corresponding author

Email addresses: jakub.houlik@fsv.cvut.cz (J. Houlík), jan.valentin@fsv.cvut.cz (J. Valentin), vaclav.nezerka@cvut.cz (V. Nežerka)

grade bitumen resulting from crude oil distillation or as a modified binder (e.g., polymer-modified bitumen) where various polymers or additives are mixed with the neat binder [1].

The fatigue life of AC is a crucial parameter that determines to a large extent the maintenance costs [2]. In this regard, AC should withstand cyclic heavy traffic loads under different environmental conditions and accommodate cumulative damage without excessive opening of cracks [3, 4]. The main driver of AC deterioration and limited capability to withstand repeated tensile stresses is the aging of the bituminous binder due to oxidation [5, 6], and the failure occurs when the material cannot withstand the applied tensile strain [7]. While cold temperatures lead to increased brittleness and, in case of freezing, ice causes the opening of cracks [8], elevated temperatures make bituminous binders more viscous and prone to flow [9].

Fatigue resistance is influenced by several factors, most notably the binder content [8], air voids content [10, 11], loading strain [12, 13], and operational temperature [13, 14]. It is typically evaluated using different laboratory methods, most commonly four-point bending, semi-circular bending, and indirect tensile tests. The four-point beam fatigue test assesses fatigue behavior under bending loads, determining fatigue life, stiffness, and strength [15–17]. The semi-circular test, similar in nature, allows, in addition, evaluation of fracture toughness [18, 19]. The indirect tensile test applies repeated tensile loads to cylindrical AC specimens using a diametral compression setup, measuring the number of cycles to failure or accumulated strain at a constant load frequency and amplitude [17, 20, 21].

Understanding the relationships between fatigue life and AC composition, climatic conditions, and loading rate is vital for a proper mix design, but extensive testing is time-consuming. The standardized testing procedures require 14–42 days for the preparation of specimens and proper drying [22], and the test itself takes from hours to several days, depending on the load level and frequency of loading. While the standardized testing methods offer valuable insights, they are time and resource-intensive. Leveraging machine learning (ML) models and already collected data, AC's fatigue life can be predicted when time-consuming testing is impossible.

Numerous studies have extensively reviewed various aspects such as the underlying mechanisms, characterization techniques, and mitigation strategies, highlighting the intricate interactions

between AC's components and the influence of external factors such as aging and environmental conditions on fatigue behavior [2, 3, 23, 24]. Recent studies on ML-assisted mix design [25–27] have laid the groundwork for developing models that integrate a broader range of variables to predict fatigue life. Still, our goal is to use a larger amount of data for ML modeling and find relationships only between the most easily evaluated properties that can be targeted during the design: binder content (%) and air voids (%). These two microstructural parameters were identified in a recent comprehensive work by Alnaqbi et al. [28] as critical variables regarding the longevity of AC pavements. To the best of our knowledge, despite the existence of ML-based models for estimating AC stiffness [29–31], the utilization of neural networks for predicting fatigue life in laboratory specimens has not been, in such extent and detailed analysis, reported in the scientific literature.

2. Methodology

Our study's methodology involved using artificial neural networks (ANNs) to predict fatigue cycle quantification in AC specimens. We based our predictions on existing datasets obtained exclusively during four-point bending tests loaded at a constant strain rate. This approach was chosen because it is widely adopted in the field, thereby ensuring the availability of an extensive and robust dataset for model training and validation.

2.1. Data collection

The data utilized to train and test the models were meticulously compiled from a wide range of peer-reviewed scientific publications, detailing essential parameters such as binder content (%), air voids (%), loading strain (ε), test temperature, loading frequency (f), and the number of cycles until failure (N_f). Our dataset exclusively comprises samples subjected to four-point bending at temperatures of 20 °C and 70 °F (21.1 °C). In total, the analysis incorporated 206 samples drawn from 4 distinct studies (Table 1). To ensure the robustness and reliability of our analysis, we applied a non-symmetric percentile-based filtering method to eliminate outliers from the fatigue life dataset. This method involved calculating the 3rd and 90th percentiles to establish lower and upper bounds of 2×10^3 and 2×10^6 , respectively, thereby excluding extreme values that could

skew the results while maintaining the core statistical properties. We also utilized a Z-score filter, which calculates the standard deviations from the mean for each variable (binder content, air voids, applied strain, and fatigue life). The Z-value threshold was set to 3.0 to ensure the exclusion of outliers further. This approach ensures that the analysis remains robust and relevant to the study’s practical constraints. This aggregation of data from various authors significantly enhances the model’s reliability, providing more accurate and robust predictions. Due to incomplete datasets in a few other studies, excluding them from the data table employed for model training became necessary.

2.2. ANN

The ANN model is highly effective for processing tabular numerical data, which makes it well-suited for fatigue life predictions. The model assigns weights to different input variables and combines them through several hidden layers to generate the output (Figure 1). These weights are adjusted based on validation data through multiple iterations to improve the model’s accuracy.

The codes developed, final models, and the data used in this study are provided as open source and can be accessed on GitHub¹.

Specifically, we developed the prediction model using the Sequential model from the Keras library, version 2.12.0rc1. Before training, the data were normalized using the *MinMaxScaler* function from the *sklearn.preprocessing* module to scale the input variables between 0 and 1. The Sequential model was configured with the following input variables (hyperparameters): number of hidden layers (n_h), number of neurons within the hidden layers ($n_{neur,h}$), the activation function, and the optimization algorithm used (Table 2). All these hyperparameters were scrutinized and optimized to reach the highest R^2 value defined as

$$R^2 = 1 - \frac{\sum_{i=1}^n (N_{f,i} - \hat{N}_{f,i})^2}{\sum_{i=1}^n (N_{f,i} - \bar{N}_f)^2}, \quad (1)$$

where $N_{f,i}$ is the measured output, $\hat{N}_{f,i}$ is the model prediction, \bar{N}_f is the mean of $N_{f,i}$, and n is the number of samples.

¹<https://github.com/VaclavNezerka/AsphaltFatigueANN>

Table 1: Summary of studies on AC fatigue measurements detailing data utilization in our modeling and reasons for exclusion of specific datasets.

| Reference | Binder content (%) | Air voids (%) | ε ($\times 10^{-6}$) | Temperature ($^{\circ}\text{C}$) | f (Hz) | N_f ($\times 10^3$) | Samples | Used for modeling |
|-----------------------------|--------------------|---------------|------------------------------------|------------------------------------|-------------|-------------------------|---------|-------------------|
| Li et al. [32] | 4.0–6.0 | 1.3–7.7 | 500–1000 | 20 | 10 | 4–1,588 | 22 | Yes |
| Witczak et al. [33] | 4.2–5.2 | 4.0–10.8 | 137–300 | 4.4, 21.1, 37.8 | 10 | 2–700 | 229 | Yes ^a |
| Pais et al. [34] | 4.7–6.5 | 1.2–12.8 | 115–800 | 20 | 10 | 3–19,500 | 115 | Yes |
| Saboo et al. [35] | 4.7–6.7 | 4.0–4.1 | 400–1000 | 20 | 10 | 1–152 | 38 | Yes |
| Ameri et al. [36] | N/A | N/A | 400–1 000 | 20 | 10 | 5–490 | 32 | No ^b |
| Al Khateeb and Ghuzian [37] | 5.1 | 4.0 | N/A | 20, 30 | 3, 5, 8, 10 | N/A | 40 | No ^c |
| Bankowski [38] | 3.7–6.3 | 2.1–4.3 | N/A | 10 | 10 | N/A | 5 | No ^c |
| Harvey et al. [39] | 4.0–6.0 | 1.2–8.9 | 150–300 | 19 | 10 | 14–1,472 | 30 | No ^c |
| Ly et al. [40] | N/A | 3.4–4.7 | N/A | 20 | 10 | 0–3,365 | 72 | No ^c |
| Maczka and Mackiewicz [41] | 3.8–4.2 | 4.0–6.2 | N/A | N/A | N/A | 149–1,958 | 12 | No ^b |
| Pakholak et al. [42] | 6.3–12.0 | 2.9–23.8 | N/A | 5, 15, 25, 35 | 10 | N/A | 96 | No ^c |
| Shen and Lu [43] | N/A | N/A | 300–1 000 | 20 | 10 | 3–446 | 5 | No ^a |
| Shu et al. [44] | 5.0–5.5 | 7.0 | 600 | 25 | 10 | 83–117 | 4 | No ^d |
| Zeiyada et al. [45] | 4.2–5.2 | 3.4–10.0 | 75–200 | 20 | 10 | 3–676 | 21 | No ^c |
| Zhang et al. [46] | 6.5–6.6 | 6.0 | 202–1 032 | 7, 13, 20 | 10 | 1–230 | 38 | No ^c |
| Zhou et al. [47] | 5.8–7.3 | 3.5–4.5 | 75–500 | 25 | 10 | 0–43,900 | 24 | No ^c |

^a Only data obtained at 70°F.

^b Missing information about binder content and air voids or temperature.

^c Different testing method than four-point bending.

^d Different testing temperature than 20°C/70°F.

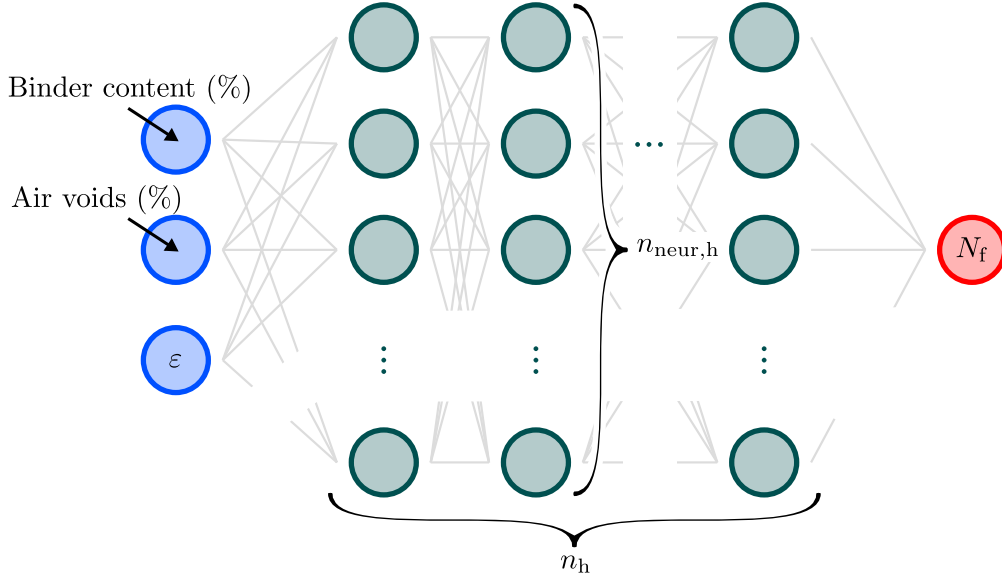


Figure 1: Scheme of the neural network architecture used for modeling, illustrating the network parameters.

The ANN was trained for 300,000 epochs to ensure a sufficient number of iterations for the learning process. Throughout the training, we focused on minimizing the loss function, ultimately saving the version of the model that achieved the lowest loss, representing the most accurate predictions without overfitting. Given the wide range of fatigue life data, which is typically represented on a logarithmic scale to accommodate its vast spread, we employed two distinct loss functions: (i) mean square error (L_{MSE}), defined as

$$L_{\text{MSE}}(N_f, \hat{N}_f) = \frac{1}{n} \sum_{i=1}^n (N_{f,i} - \hat{N}_{f,i})^2, \quad (2)$$

and (ii) mean square logarithmic error (L_{MSLE}), defined as

$$L_{\text{MSLE}}(N_f, \hat{N}_f) = \frac{1}{n} \sum_{i=1}^n (\log(N_{f,i} + 1) - \log(\hat{N}_{f,i} + 1))^2. \quad (3)$$

This strategic choice aimed to optimize our models for the logarithmic nature of fatigue life variability. Employing both L_{MSE} and L_{MSLE} as loss functions enabled us to fine-tune the model's sensitivity to the scale of the data.

To validate the robustness and reliability of our ANN model, we employed cross-validation

Table 2: Hyperparameters tested during the model development and values selected for the final model.

| Hyperparameter | Grid | Selected |
|---------------------|-----------------------|----------|
| Loss function | L_{MSE}, L_{MSE} | both |
| Optimizer | Adam, Nadam, RMSprop | RMSprop |
| Activation function | ReLU, Linear, Sigmoid | ReLU |
| n_h | 1, 2, 3, 4 | 2 |
| $n_{neur,h}$ | 10, 50, 100, 150, 200 | 200 |

techniques during its training and testing phases. Cross-validation was essential to ensure that the model performed well regardless of how the data was divided. We implemented this by dividing the dataset into four distinct folds, using the *sklearn.model_selection.KFold* class. In each cross-validation cycle, one fold was designated for testing, while the remaining three folds were used for training. This process was iterated across all folds, mitigating the risk of overfitting specific data subsets. We opted for four-fold cross-validation to balance computational efficiency and the risk of having too few data points in each fold, ensuring a comprehensive evaluation. Additionally, the dataset was shuffled before splitting with the *KFold* function, guaranteeing a randomized and uniform distribution of data across all folds.

The modeling and subsequent training were carried out on a Dell XPS 9370 notebook with the following specifications: Intel(R) Core(TM) i7-8550U CPU (1.80GHz), 16 GB RAM, PM981 NVMe Samsung SSD hard drive, and Windows 11 operating system. The code was developed in Python, version 3.10.14. With such hardware, training a single model for 300,000 epochs took between 1 and 2 hours.

3. Results and discussion

3.1. Hyperparameters

Before the thorough process of optimizing the hyperparameters for the ANN model, we initially explored various configurations, promptly identifying that the ReLU activation function outperformed other options. This preference for ReLU and selection of the Adam optimizer stems from their inherent characteristics: ReLU’s ability to mitigate the vanishing gradient problem [48], thus ensuring a more effective backpropagation of errors through the network and Adam’s adaptive

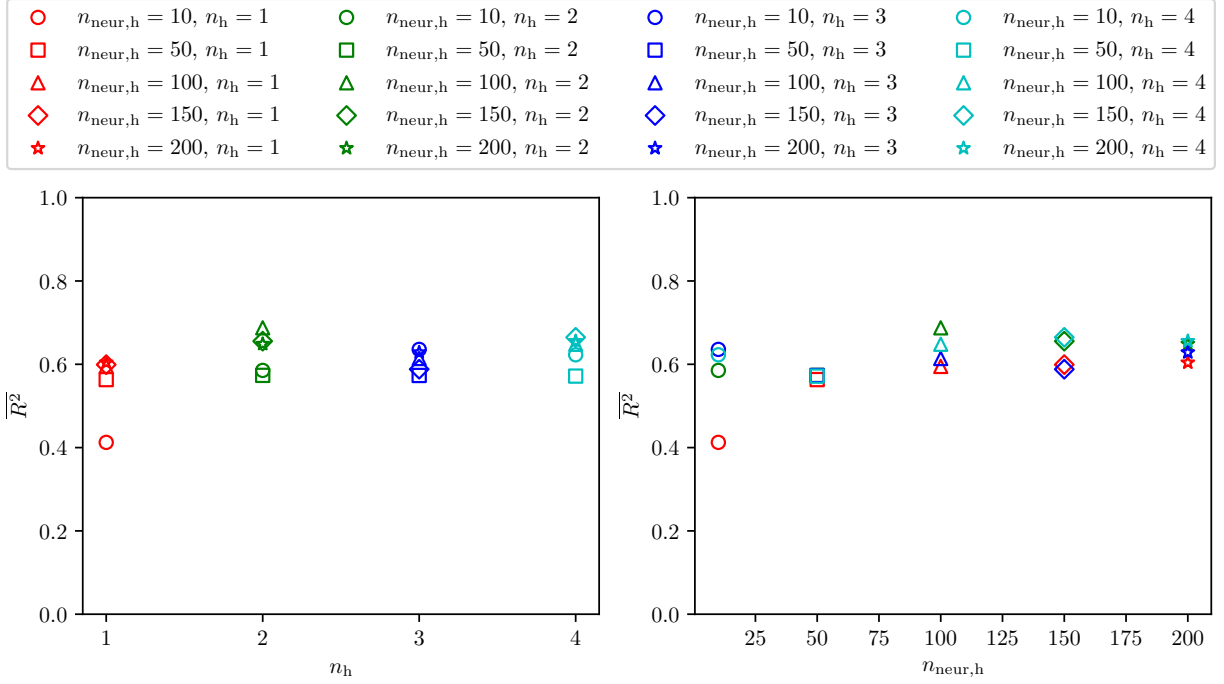


Figure 2: Variation of the model performance, measured by the $\overline{R^2}$ score (mean for different folds), in relation to n_h (left) and $n_{neur,h}$ (right) when employing L_{MSE} as the loss function; RMSprop optimizer and ReLU activation function.

learning rate effectively fine-tuning the weights [49]. Guided by these insights, we conducted a detailed examination to determine the optimal settings for n_h and $n_{neur,h}$, testing these configurations against both L_{MSE} and L_{MSLE} loss functions (Figures 2 and 3, respectively). This analysis revealed that a structure with $n_h = 2$ and $n_{neur,h} = 200$ achieved the highest $\overline{R^2}$ score after averaging the R^2 score of all four folds.

Subsequent evaluations of various activation functions under this configuration affirmed that ReLU was the superior choice. Linear activation functions led to compromised predictions, while sigmoid and tanh resulted in $\overline{R^2} < 0$, indicating inadequate model performance. This outcome underscores ReLU’s advantage in maintaining non-linearity in deep networks, which is crucial for tackling fatigue life prediction.

When comparing the efficacy of different optimizers, while the impact was less pronounced, the RMSprop (root mean square propagation) optimizer consistently showed superior performance

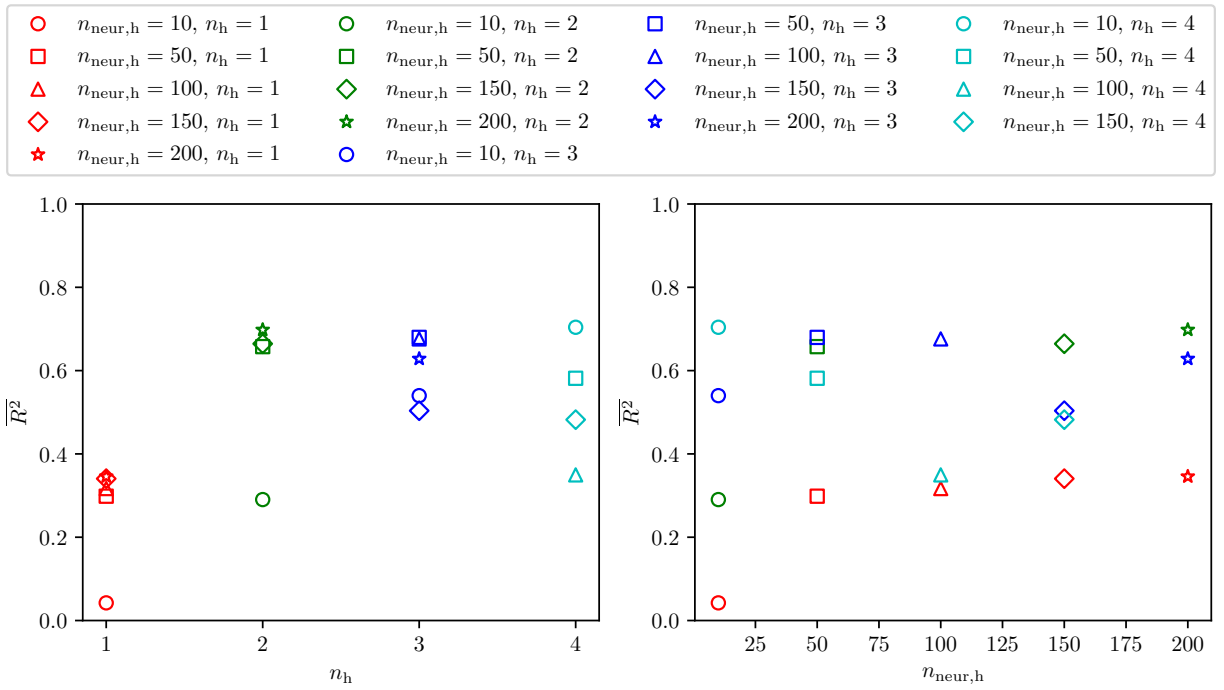


Figure 3: Variation of the model performance, measured by the $\overline{R^2}$ score (mean for different folds), in relation to n_h (left) and $n_{\text{neur},h}$ (right) when employing L_{MSLE} as the loss function; RMSprop optimizer and ReLU activation function. Some configurations did not lead to the model convergence and are therefore excluded from the results.

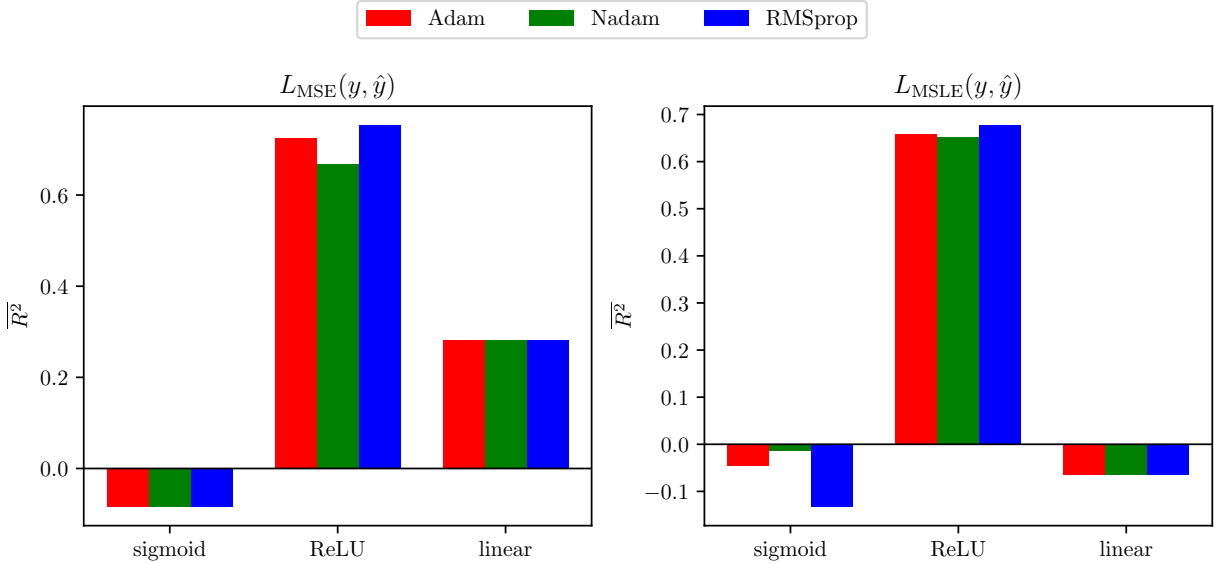


Figure 4: Model performance, measured by the $\overline{R^2}$ score (mean for different folds), in relation to the activation functions and optimizers used, when employing L_{MSE} (left) and L_{MSLE} (right) as the loss functions; $n_h = 2$ and $n_{neur,h} = 100$ (L_{MSE}) and $n_h = 2$ and $n_{neur,h} = 200$ (L_{MSLE}).

when using the ReLU activation function for both L_{MSE} and L_{MSLE} (Figure 4). RMSprop adjusts the learning rate by using a moving average of the squared gradients, providing stability in noisy data environments by smoothing out the updates [50]. On the other hand, Nadam, which integrates Nesterov momentum into the Adam optimizer’s structure, speeds up the model updates [51]. This approach can sometimes overshoot the smallest or optimal values or struggle to stabilize on complex, uneven loss surfaces. While sometimes yielding faster convergence, this aggressive update strategy can lead to instability and lower R^2 scores, mainly when dealing with non-uniform data distributions or outliers.

3.2. Model accuracy

Training convergence was more effectively achieved with L_{MSE} (Figure 5). This smooth convergence results from the linearity of L_{MSE} , simplifying the optimization of model weights. In contrast, L_{MSLE} , which introduces a logarithmic transformation to the loss calculation, presented challenges in convergence. The non-linear scaling of MSLE complicates the optimization process, as it adjusts the error contributions in a non-uniform manner, making it more difficult to fine-tune

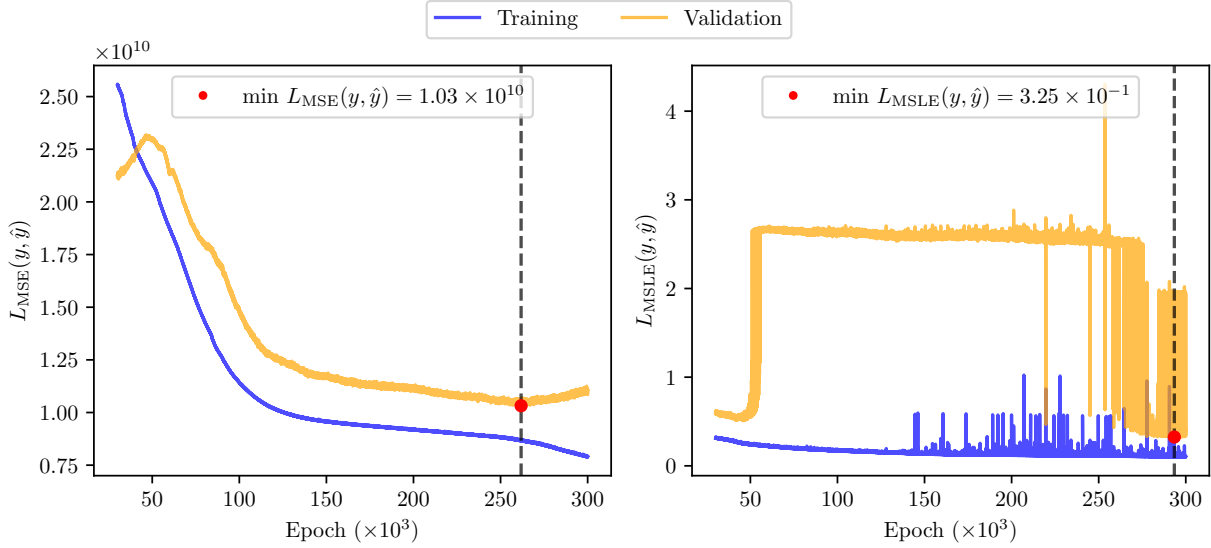


Figure 5: Training convergence plots illustrating the progression of the training process over 300,000 epochs for both L_{MSE} (left) and L_{MSLE} (right).

the model’s weights accurately. The models reached optimal performance for both loss functions between 250,000 and 300,000 epochs.

Upon comparing the models’ performance with the entire dataset (Figure 6), both approaches yielded similar R^2 scores, 0.895 for L_{MSE} and 0.896 for L_{MSLE} . However, training with the linear loss function resulted in less accurate predictions for samples with N_f below approximately 2×10^5 . This discrepancy was evident in the scatter from the line of equality in the true versus predicted plot, indicating a more significant variance in predictions for lower N_f values. This variation results from the logarithmic nature of the N_f data, supporting the use of L_{MSLE} for such distributions.

3.3. Practical outcomes

Further analysis involved generating partial dependence plots (Figures 7 and 8) to explore the relationships between input parameters and predicted N_f values for both models. These plots were constructed while adhering closely to the scatter distribution of the input data to avoid extrapolation, which could yield unreliable results; the input data points are marked with white triangular markers. Predictions were executed at two strain levels, 200×10^{-6} and 400×10^{-6} , revealing that a lower air voids content (ideally below 3%) correlates with an extended fatigue life. Similarly, an

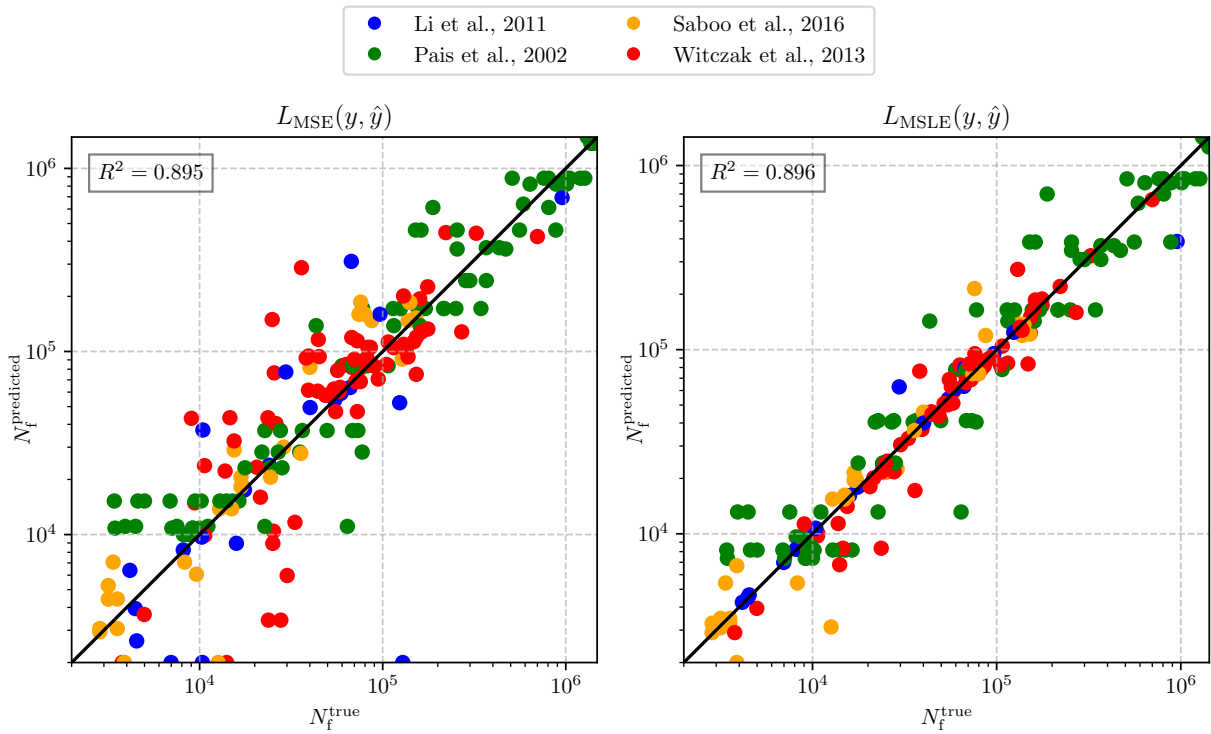


Figure 6: Comparison of true versus predicted values for the entire dataset when using L_{MSE} (left) and L_{MSLE} (right).

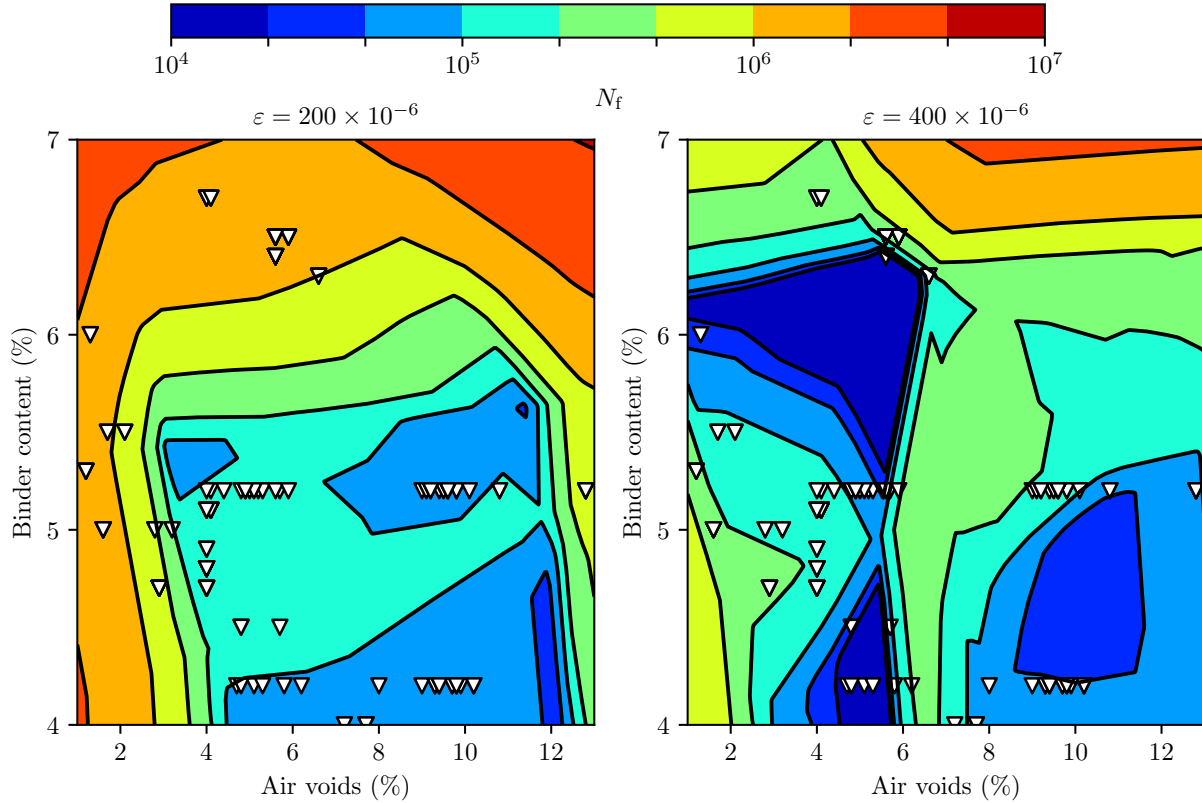


Figure 7: Partial dependence plots generated using the calibrated model trained with L_{MSE} , showing the relationship between input parameters and predicted N_f at two different strain levels; input data points are indicated by white triangular markers.

increase in binder content was found to enhance fatigue life, with L_{MSLE} -based models indicating that high binder levels (over 6%) could mitigate the adverse effects of high air voids content.

Both models agree that a high air-void content combined with a low binder content results in AC with inferior fatigue life. These findings suggest that durable AC should contain at least 6% bituminous binder. While the models indicate that higher air void content could be advantageous when combined with high binder content, this scenario falls outside the coverage of the input data, leading to extrapolation by the models in this region and, therefore, unreliable data that need to be further verified experimentally.

These findings are in agreement with the study by Zeiada et al. [45], who reported higher N_f by approximately factor of 3 after increasing the binder content from 4.2% to 5.2% but increasing

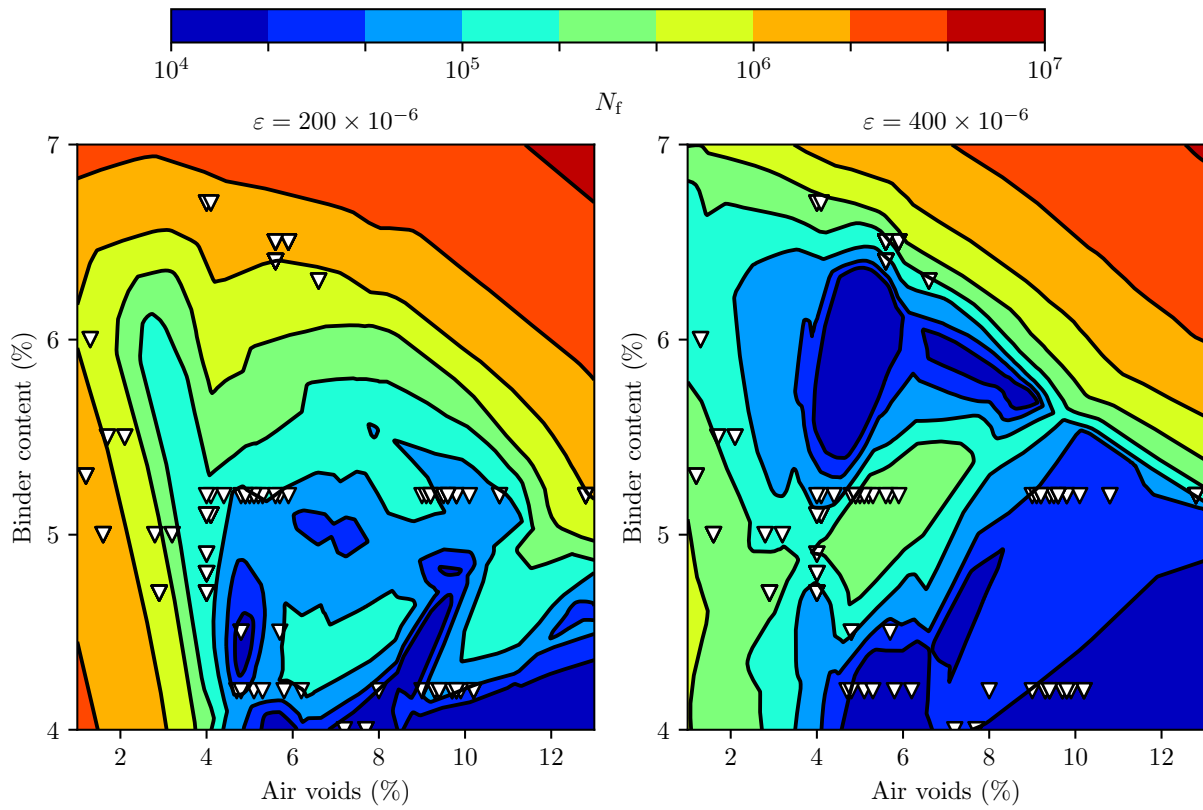


Figure 8: Partial dependence plots generated using the calibrated model trained with L_{MSLE} , showing the relationship between input parameters and predicted N_f at two different strain levels; input data points are indicated by white triangular markers.

the content of air voids from 4.5% to 9.5% resulted in relatively similar results on average, only exhibiting a higher variability. This phenomenon was scrutinized by Ma et al. [52], who proved in their numerical model that AC specimens having the same air voids content can exhibit different fatigue life due to the non-uniform distribution of air voids. A conference paper by Yan et al. [53] reports on constructing an ANN for N_f prediction. In their study, the crucial parameters about samples, testing conditions, and the model are missing; however, even their experimental data indicate that the fatigue life of AC is not impacted significantly by air voids while increasing binder content leads to higher N_f values.

4. Conclusion

The study employed artificial neural networks (ANNs) to predict the fatigue life of asphalt concrete (AC), focusing on the impact of strain level, binder content, and air voids. Utilizing a substantial dataset, we tailored the ANN models to accommodate the wide range of fatigue life data, represented typically on a logarithmic scale. Our strategic use of both mean square error (L_{MSE}) and mean square logarithmic error (L_{MSLE}) as loss functions allowed for fine-tuning the model's sensitivity to the scale of the data, addressing the logarithmic distribution of fatigue life.

Through rigorous hyperparameter optimization, we identified that a model architecture with two hidden layers containing 200 neurons provided the best performance. The ReLU activation function proved optimal, and the RMSprop optimizer emerged as the most stable.

Our evaluation demonstrated that L_{MSE} generally facilitated better training convergence due to its straightforward linearity. However, L_{MSLE} was indispensable for capturing the variability in lower ranges of fatigue life data, as evidenced by the close R^2 scores of 0.895 for L_{MSE} and 0.896 for L_{MSLE} , yet with more consistent predictions across the logarithmic scale.

The detailed analysis of the developed models revealed critical insights into the relationships between AC's microstructural parameters and fatigue life. Lower air-void and higher binder content were associated with extended fatigue life. However, high air-void and low binder content markedly reduced fatigue life, underscoring the critical balance needed for durable AC. Such findings highlight the importance of optimizing binder and air-void content in AC mix design to improve pavement durability and reduce maintenance costs.

This research not only underscores the capabilities of ANNs in predicting AC fatigue life but also sets a foundation for using more extensive datasets in future modeling efforts. It offers valuable guidance on the interplay between AC's fundamental properties and performance, paving the way for more informed and effective pavement engineering practices.

Funding. This work was supported by the Czech Science Foundation (no. 22-04047K) and the Czech Technical University in Prague, grant agreement (no. SGS24/003/OHK1/1T/11). V. Nežerka's contribution was funded by the European Union under the project ROBOPROX (no. CZ.02.01.01/00/22_008/0004590)

References

- [1] J. Valentin, J. Trejbal, V. Nežerka, T. Valentová, P. Vacková, P. Tichá, A comprehensive study on adhesion between modified bituminous binders and mineral aggregates, *Construction and Building Materials* 305 (2021) 124686. [doi:10.1016/j.conbuildmat.2021.124686](https://doi.org/10.1016/j.conbuildmat.2021.124686).
- [2] M. M. Isied, M. I. Souliman, Integrated predictive artificial neural network fatigue endurance limit model for asphalt concrete pavements, *Canadian Journal of Civil Engineering* 46 (2019) 114–123. [doi:10.1139/cjce-2018-0051](https://doi.org/10.1139/cjce-2018-0051).
- [3] F. Xiao, S. Amirkhanian, C. H. Juang, Prediction of fatigue life of rubberized asphalt concrete mixtures containing reclaimed asphalt pavement using artificial neural networks, *Journal of Materials in Civil Engineering* 21 (2009) 253–261. [doi:10.1061/\(asce\)0899-1561\(2009\)21:6\(253\)](https://doi.org/10.1061/(asce)0899-1561(2009)21:6(253)).
- [4] B. Shi, Q. Dong, X. Chen, X. Gu, X. Wang, S. Yan, A comprehensive review on the fatigue resistance of recycled asphalt materials: Influential factors, correlations and improvements, *Construction and Building Materials* 384 (2023) 131435. [doi:10.1016/j.conbuildmat.2023.131435](https://doi.org/10.1016/j.conbuildmat.2023.131435).
- [5] C. A. Bell, D. Sosnovske, J. Wieder, Aging: binder validation, Strategic Highway Research Program, National Research Council Washington, DC, 1994.

- [6] S. Sreedhar, E. Coleri, The effect of long-term aging on fatigue cracking resistance of asphalt mixtures, *International Journal of Pavement Engineering* 23 (2020) 308–320. doi:10.1080/10298436.2020.1745206.
- [7] N. D. Beskou, S. V. Tsinopoulos, G. D. Hatzigeorgiou, Fatigue cracking failure criterion for flexible pavements under moving vehicles, *Soil Dynamics and Earthquake Engineering* 90 (2016) 476–479. doi:10.1016/j.soildyn.2016.09.019.
- [8] E. Maczka, P. Mackiewicz, Asphalt mixtures fatigue life considering various environmental impacts, *Materials* 16 (2023) 966. doi:10.3390/ma16030966.
- [9] F. Moreno-Navarro, M. Sol-Sánchez, G. García-Travé, M. C. Rubio-Gámez, Fatigue cracking in asphalt mixtures: the effects of ageing and temperature, *Road Materials and Pavement Design* 19 (2017) 561–570. doi:10.1080/14680629.2018.1418717.
- [10] A. J. Enríquez-León, T. D. de Souza, F. T. S. Aragão, D. Braz, A. M. B. Pereira, L. P. Nogueira, Determination of the air void content of asphalt concrete mixtures using artificial intelligence techniques to segment micro-CT images, *International Journal of Pavement Engineering* 23 (2021) 3973–3982. doi:10.1080/10298436.2021.1931197.
- [11] F. Praticò, A. Moro, Measurement of air void content in hot mix asphalts: Method and core diameter dependence, *Construction and Building Materials* 26 (2012) 344–349. doi:10.1016/j.conbuildmat.2011.06.032.
- [12] M.-C. Liao, J.-S. Chen, K.-W. Tsou, Fatigue characteristics of bitumen-filler mastics and asphalt mixtures, *Journal of Materials in Civil Engineering* 24 (2012) 916–923. doi:10.1061/(asce)mt.1943-5533.0000450.
- [13] Y. Zhang, J. Zhang, T. Ma, H. Qi, C. Chen, Predicting asphalt mixture fatigue life via four-point bending tests based on viscoelastic continuum damage mechanics, *Case Studies in Construction Materials* 19 (2023) e02671. doi:10.1016/j.cscm.2023.e02671.

- [14] K. Yang, H. Cui, X. Ma, M. Zhu, Understanding and characterizing the fatigue cracking resistance of asphalt binder at intermediate temperature: A literature review, *Construction and Building Materials* 407 (2023) 133432. doi:10.1016/j.conbuildmat.2023.133432.
- [15] H. Cheng, J. Liu, L. Sun, L. Liu, Y. Zhang, Fatigue behaviours of asphalt mixture at different temperatures in four-point bending and indirect tensile fatigue tests, *Construction and Building Materials* 273 (2021) 121675. doi:10.1016/j.conbuildmat.2020.121675.
- [16] H. Cheng, L. Sun, Y. Wang, L. Liu, X. Chen, Fatigue test setups and analysis methods for asphalt mixture: A state-of-the-art review, *Journal of Road Engineering* 2 (2022) 279–308. doi:10.1016/j.jreng.2022.11.002.
- [17] N. Sudarsanan, Y. R. Kim, A critical review of the fatigue life prediction of asphalt mixtures and pavements, *Journal of Traffic and Transportation Engineering (English Edition)* 9 (2022) 808–835. doi:10.1016/j.jtte.2022.05.003.
- [18] G. Saha, K. P. Biligiri, Fracture damage evaluation of asphalt mixtures using semi-circular bending test based on fracture energy approach, *Engineering Fracture Mechanics* 142 (2015) 154–169. doi:10.1016/j.engfracmech.2015.06.009.
- [19] P. Zielinski, The use of the semi-circular bending method to assess the intermediate-temperature fracture toughness of asphalt concrete mixes with reclaimed asphalt shingles, *Road Materials and Pavement Design* 25 (2023) 81–98. doi:10.1080/14680629.2023.2194432.
- [20] M. T. Nguyen, H. J. Lee, J. Baek, Fatigue analysis of asphalt concrete under indirect tensile mode of loading using crack images, *Journal of Testing and Evaluation* 41 (2012) 104589. doi:10.1520/jte104589.
- [21] T. Vishnu, Laboratory investigation on the fatigue performance of asphalt mixes reinforced with human hair fiber in pavement application, *Materials Today: Proceedings* doi:10.1016/j.matpr.2023.01.070.

- [22] CEN, EN 12697-24: 2018; Bituminous Mixtures—Test Methods—Part 24: Resistance to Fatigue, European Standard.
- [23] Z. Wang, D. Liu, B. Hu, C. Zhu, W. Luo, An improved regression model to predict fatigue life of asphalt mixes incorporating low to moderate RAP contents, *Construction and Building Materials* 374 (2023) 130904. [doi:10.1016/j.conbuildmat.2023.130904](https://doi.org/10.1016/j.conbuildmat.2023.130904).
- [24] R. Lundstrom, H. D. Benedetto, U. Isacsson, Influence of asphalt mixture stiffness on fatigue failure, *Journal of Materials in Civil Engineering* 16 (2004) 516–525. [doi:10.1061/\(asce\)0899-1561\(2004\)16:6\(516\)](https://doi.org/10.1061/(asce)0899-1561(2004)16:6(516)).
- [25] J. Chen, Y. Liu, Fatigue modeling using neural networks: A comprehensive review, *Fatigue & Fracture of Engineering Materials & Structures* 45 (2022) 945–979. [doi:10.1111/ffe.13640](https://doi.org/10.1111/ffe.13640).
- [26] R. Hooda, V. Joshi, M. Shah, A comprehensive review of approaches to detect fatigue using machine learning techniques, *Chronic Diseases and Translational Medicine* 8 (2022) 26–35. [doi:10.1016/j.cdtm.2021.07.002](https://doi.org/10.1016/j.cdtm.2021.07.002).
- [27] Z. Lian, M. Li, W. Lu, Fatigue life prediction of aluminum alloy via knowledge-based machine learning, *International Journal of Fatigue* 157 (2022) 106716. [doi:10.1016/j.ijfatigue.2021.106716](https://doi.org/10.1016/j.ijfatigue.2021.106716).
- [28] A. J. Alnaqbi, W. Zeiada, G. Al-Khateeb, A. Abttan, M. Abuzwidah, Predictive models for flexible pavement fatigue cracking based on machine learning, *Transportation Engineering* 16 (2024) 100243. [doi:10.1016/j.treng.2024.100243](https://doi.org/10.1016/j.treng.2024.100243).
- [29] G. S. Moussa, M. Owais, Pre-trained deep learning for hot-mix asphalt dynamic modulus prediction with laboratory effort reduction, *Construction and Building Materials* 265 (2020) 120239. [doi:10.1016/j.conbuildmat.2020.120239](https://doi.org/10.1016/j.conbuildmat.2020.120239).
- [30] G. S. Moussa, M. Owais, Modeling hot-mix asphalt dynamic modulus using deep residual neural networks: Parametric and sensitivity analysis study, *Construction and Building Materials* 294 (2021) 123589. [doi:10.1016/j.conbuildmat.2021.123589](https://doi.org/10.1016/j.conbuildmat.2021.123589).

- [31] I. D. Uwanuakwa, A. Busari, S. I. A. Ali, M. R. Mohd Hasan, A. Sani, S. I. Abba, Comparing machine learning models with Witczak NCHRP 1-40D model for hot-mix asphalt dynamic modulus prediction, *Arabian Journal for Science and Engineering* 47 (2022) 13579–13591. [doi:10.1007/s13369-022-06935-x](https://doi.org/10.1007/s13369-022-06935-x).
- [32] Q. Li, H. J. Lee, T. W. Kim, A simple fatigue performance model of asphalt mixtures based on fracture energy, *Construction and Building Materials* 27 (2012) 605–611. [doi:10.1016/j.conbuildmat.2011.07.001](https://doi.org/10.1016/j.conbuildmat.2011.07.001).
- [33] M. Witczak, M. Mamlouk, M. Souliman, W. Zeiada, Validating an Endurance Limit for Hot-Mix Asphalt (HMA) Pavements: Laboratory Experiment and Algorithm Development (project no. NCHRP 9-44 A, 2013).
- [34] J. Pais, P. Pereira, L. Picado-Santos, Variability of laboratory fatigue life of asphalt mixes using four point bending test results, Department of Civil Engineering, University of Minho, Portugal., *IPJ* 1 (2).
- [35] N. Saboo, B. P. Das, P. Kumar, New phenomenological approach for modeling fatigue life of asphalt mixes, *Construction and Building Materials* 121 (2016) 134–142. [doi:10.1016/j.conbuildmat.2016.05.147](https://doi.org/10.1016/j.conbuildmat.2016.05.147).
- [36] M. Ameri, S. Nowbakht, M. Molayem, M. H. Mirabimoghaddam, A study on fatigue modeling of hot mix asphalt mixtures based on the viscoelastic continuum damage properties of asphalt binder, *Construction and Building Materials* 106 (2016) 243–252. [doi:10.1016/j.conbuildmat.2015.12.066](https://doi.org/10.1016/j.conbuildmat.2015.12.066).
- [37] K. A. G. Ghazi G. Al-Khateeb, The combined effect of loading frequency, temperature, and stress level on the fatigue life of asphalt paving mixtures using the idt test configuration, *International Journal of Fatigue* 59 (2014) 254–261. [doi:https://doi.org/10.1016/j.ijfatigue.2013.08.011](https://doi.org/10.1016/j.ijfatigue.2013.08.011).
- [38] W. Bańkowski, Evaluation of fatigue life of asphalt concrete mixtures with reclaimed asphalt pavement, *Applied Sciences* 8 (2018) 469. [doi:10.3390/app8030469](https://doi.org/10.3390/app8030469).

- [39] J. T. Harvey, J. A. Deacon, B.-W. Tsai, C. L. Monismith, Fatigue performance of asphalt concrete mixes and its relationship to asphalt concrete pavement performance in California, University of California Berkeley, Institute of Transportation Studies, 1995.
- [40] S. Lv, Z. Wang, X. Zhu, J. Yuan, X. Peng, Research on strength and fatigue properties of asphalt mixture with different gradation curves, *Construction and Building Materials* 364 (2023) 129872. [doi:10.1016/j.conbuildmat.2022.129872](https://doi.org/10.1016/j.conbuildmat.2022.129872).
- [41] E. Maczka, P. Mackiewicz, Asphalt mixtures fatigue life considering various environmental impacts, *Materials* 16 (2023) 966. [doi:10.3390/ma16030966](https://doi.org/10.3390/ma16030966).
- [42] R. Pakholak, A. Plewa, W. Gardziejczyk, Influence of type of modified binder on stiffness and rutting resistance of low-noise asphalt mixtures, *Materials* 14 (2021) 2884. [doi:10.3390/ma14112884](https://doi.org/10.3390/ma14112884).
- [43] S. Shen, X. Lu, Energy based laboratory fatigue failure criteria for asphalt materials, *Journal of Testing and Evaluation* 39 (2011) 313–320. [doi:10.1520/jte103088](https://doi.org/10.1520/jte103088).
- [44] X. Shu, B. Huang, D. Vukosavljevic, Laboratory evaluation of fatigue characteristics of recycled asphalt mixture, *Construction and Building Materials* 22 (2008) 1323–1330. [doi:10.1016/j.conbuildmat.2007.04.019](https://doi.org/10.1016/j.conbuildmat.2007.04.019).
- [45] W. A. Zeiada, K. E. Kaloush, B. S. Underwood, M. S. Mamlouk, Effect of Air Voids and Asphalt Content on Fatigue Damage Using the Viscoelastic Continuum Damage Analysis, American Society of Civil Engineers, 2013. [doi:10.1061/9780784413005.094](https://doi.org/10.1061/9780784413005.094).
- [46] J. Zhang, M. Sabouri, M. N. Guddati, Y. R. Kim, Development of a failure criterion for asphalt mixtures under fatigue loading, *Road Materials and Pavement Design* 14 (2013) 1–15. [doi:10.1080/14680629.2013.812843](https://doi.org/10.1080/14680629.2013.812843).
- [47] F. Zhou, W. Mogawer, H. Li, A. Andriescu, A. Copeland, Evaluation of fatigue tests for characterizing asphalt binders, *Journal of Materials in Civil Engineering* 25 (2013) 610–617. [doi:10.1061/\(asce\)mt.1943-5533.0000625](https://doi.org/10.1061/(asce)mt.1943-5533.0000625).

- [48] A. Jentzen, A. Riekert, Convergence analysis for gradient flows in the training of artificial neural networks with ReLU activation, *Journal of Mathematical Analysis and Applications* 517 (2023) 126601. doi:10.1016/j.jmaa.2022.126601.
- [49] D. P. Kingma, J. Ba, [Adam: A method for stochastic optimization](#), in: Y. Bengio, Y. LeCun (Eds.), 3rd International Conference on Learning Representations, ICLR 2015, San Diego, CA, USA, May 7-9, 2015, Conference Track Proceedings, 2015.
URL <http://arxiv.org/abs/1412.6980>
- [50] Y.-L. Peng, W.-P. Lee, Practical guidelines for resolving the loss divergence caused by the root-mean-squared propagation optimizer, *Applied Soft Computing* 153 (2024) 111335. doi:10.1016/j.asoc.2024.111335.
- [51] W. Cheng, X. Yang, B. Wang, W. Wang, Unbiased quasi-hyperbolic nesterov-gradient momentum-based optimizers for accelerating convergence, *World Wide Web* 26 (2022) 1323–1344. doi:10.1007/s11280-022-01086-3.
- [52] T. Ma, Y. Zhang, D. Zhang, J. Yan, Q. Ye, Influences by air voids on fatigue life of asphalt mixture based on discrete element method, *Construction and Building Materials* 126 (2016) 785–799. doi:10.1016/j.conbuildmat.2016.09.045.
- [53] C. Yan, R. Gao, W. Huang, Asphalt mixture fatigue life prediction model based on neural network, in: CICTP 2017, American Society of Civil Engineers, 2018. doi:10.1061/9780784480915.136.